



Development of platinum-based bimodal pore catalyst for CO₂ reforming of CH₄

Kai Tao^b, Yi Zhang^{a,*}, Soichiro Terao^b, Noritatsu Tsubaki^{b,**}

^a Research Center of the High Gravity Engineering and Technology, Beijing University of Chemical Technology, Beijing 100029, PR China

^b Department of Applied Chemistry, School of Engineering, University of Toyama, Gofuku 3190, Toyama 930-8555, Japan

ARTICLE INFO

Article history:

Available online 25 March 2010

Keywords:

Bimodal pore support
Platinum catalyst
Methane dry reforming
ZrO₂
Al₂O₃

ABSTRACT

The synthesis and preparation conditions for bimodal pore catalyst support were studied. SiO₂–SiO₂, ZrO₂–SiO₂, or Al₂O₃–SiO₂ bimodal pore support could be optimally prepared by incipient-wetness impregnation (IWI) of silica Q-50 pellet with silica, zirconia or alumina sol, respectively. Pore size measurement results suggested that the obtained bimodal pore supports showed two kinds of pores, mesopores and original macropores, simultaneously. The newly formed mesopores contributed to the increased BET surface area of bimodal pore support, compared with that of the original silica Q-50. Pt catalysts supported on these kinds of supports were tested in CO₂ reforming of CH₄. The performances of Pt/ZrO₂–SiO₂ and Pt/Al₂O₃–SiO₂ bimodal pore catalysts were better. Furthermore, it was found that Pt/Al₂O₃–SiO₂ bimodal catalyst showed better reforming performance than Pt/ZrO₂–SiO₂ bimodal catalyst. And furthermore, CeO₂ modified Pt/Al₂O₃–SiO₂ bimodal pore catalyst exhibited highest activity and stability under the present study conditions.

© 2010 Elsevier B.V. All rights reserved.

1. Introduction

Many industrial solid catalysts employ appropriate supports to disperse active metal or metal compounds. The role of support is not limited to maintain the catalytically active phase at a highly dispersed state; it may also contribute to catalytic activity due to chemical effect or the interaction between the active phase and the support phase. The advantage of a support with large surface area (such as silica or alumina) is that active phase can be dispersed well throughout the pore system, thus making possible to obtain a large active surface area per unit weight used. But, a support with large surface area usually consists of small pores, which is not beneficial to the diffusion of reactants or products. On the other hand, a support with large pores will facilitate the intra-pellet diffusion, but against the high dispersion of active phase, limited by its small surface area. A bimodal pore support containing mesopores and macropores, simultaneously, will show great application potential in solid catalytic reaction. Catalysts prepared by supporting metal or metal compound active phase on this kind of bimodal pore support are expected to exhibit good performance. Because, the macropores of bimodal pore support provide a rapid access to/from active phase for the reactants/products, while the mesopores of bimodal pore support offer a large surface area to well disperse the active phase. By using strong corrosive acid [1]

or organic solvents [2], SiO₂–SiO₂ or Al₂O₃–Al₂O₃ bimodal catalyst support was prepared. But, a lot of waste water was generated during the preparation process. Furthermore, only homogeneous oxide, i.e. one component bimodal pore support was obtained.

A novel way of preparing SiO₂–SiO₂ bimodal pore support by simply introducing silica nano-particles into silica macropores was reported by Tsubaki et al. [3]. The prepared cobalt supported SiO₂–SiO₂ bimodal pore catalyst showed better performance in liquid-phase Fischer–Tropsch synthesis (FTS) reaction, when compared with unimodal cobalt/silica catalysts. It was proved that the pore diffusion resistance in bimodal catalyst was not strong according to the simulation of pore diffusion model of SiO₂–SiO₂ bimodal pore catalyst for FTS [4]. Besides SiO₂, by introducing hetero-oxide sol, such as, zirconia or alumina, ZrO₂–SiO₂ or Al₂O₃–SiO₂ bimodal pore support can be prepared. These kinds of support were excellent supports for cobalt in FTS. Besides the spatial effect of bimodal pore structure, the introduced ZrO₂, or Al₂O₃ was also a promoter for the reaction with the hetero-atom combination [5,6].

Methane reforming is the first step of GTL (gas to liquid) process. CO₂ reforming of methane (dry reforming) has the advantage in utilization of raw natural gas or biogas rich in CO₂, because there is no need for CH₄/CO₂ separation. The synthesis gas produced through this process with low H₂/CO ratio (H₂/CO = 1/1) is a desirable feed for FTS on Fe-based catalyst, dimethyl ether synthesis and carbonyl synthesis [7]. Besides, this reaction is also of great environmental impacts, two kinds of greenhouse gases can be converted into valuable feed gas, simultaneously.



* Corresponding author.

** Corresponding author. Fax: +81 76 445 6848.

E-mail addresses: yizhang@mail.buct.edu.cn (Y. Zhang), tsubaki@eng.u-toyama.ac.jp (N. Tsubaki).

Transition metals (Ni, Pt, Rh, Ru) have been shown to exhibit a good activity for methane dry reforming. Nickel-based catalysts have been widely used in reforming reaction as they are relatively cheap and high activity. However, the rapid deactivation of nickel catalysts due to sintering and/or coke deposition restricts its application. Generally, there is an agreement that noble metal catalysts demonstrate lower degree of carbon deposition compared with nickel catalysts, but their activity and stability depends strongly on the property of the support [8]. Rh catalyst can maintain high activity and stability at the same time. But, platinum is preferred due to its relative low price and good availability with respect to rhodium.

In our previous work, bimodal pore catalysts were well studied in liquid phase FTS reaction. Actually, Knudsen diffusion of gaseous reactant is predominant in gas phase reaction. For liquid phase reaction, reactant diffusion inside catalyst pores makes reactant molecules having collisions with liquid medium molecules before being able to have contact with inner wall of catalyst nano-pores, more difficult to realize the advantage effect of bimodal structure directly. So, it is expected that bimodal pore catalyst will show advantage effect over unimodal pore catalyst in gas phase reaction more easily than in liquid phase reaction. Recently, we developed Pt-based bimodal pore catalyst and applied it in methane reforming reaction. Our results indicated that bimodal pore catalyst exhibited better performance, when compared with unimodal pore catalysts. Development of bimodal pore catalyst is very meaningful from the GTL industry point of view as it is possible to downsize the scale of methane reformer using catalysts with enhanced diffusion efficiency inside catalyst pores. The present work is a study of supported Pt bimodal pore catalysts for methane dry reforming ($\text{CO}_2 + \text{CH}_4$). In the present contribution, $\text{SiO}_2\text{--SiO}_2$, $\text{Al}_2\text{O}_3\text{--SiO}_2$ and $\text{ZrO}_2\text{--SiO}_2$ bimodal pore supports were prepared. Platinum was supported on these kinds of bimodal pore supports. The synthesis condition for bimodal pore support was studied. The performance of Pt/ $\text{ZrO}_2\text{--SiO}_2$ and Pt/ $\text{Al}_2\text{O}_3\text{--SiO}_2$ bimodal pore catalysts was also comparatively investigated.

2. Experimental

2.1. Catalyst preparation

The bimodal pore support was prepared by impregnation of a commercially available silica gel (Cariact Q-50, Fuji Silysia Co., specific surface area: $94\text{ m}^2/\text{g}$, pore volume: 1.35 ml/g , pellet size in diameter: $75\text{--}500\text{ }\mu\text{m}$ and pore diameter: 59 nm), with silica sol (Snowtex XS, Nissan Chemicals Co., particle size in diameter: 5 nm , solid content: $21\text{ wt}\%$, aqueous solution), zirconia sol (Ceramic G-401, Nibban Institute Co., particle size in diameter: $1.7\text{--}2.4\text{ nm}$, solid content: 16% , alcohol solution) or alumina sol (Alumina sol 520, Nissan Chemicals Co., particle size in diameter: $5\text{--}6\text{ nm}$, solid content: $20\text{ wt}\%$, aqueous solution). After the impregnation, the support was calcined in air at a given temperature for 2 h directly to prepare $\text{SiO}_2\text{--SiO}_2$, $\text{Al}_2\text{O}_3\text{--SiO}_2$ and $\text{ZrO}_2\text{--SiO}_2$ bimodal pore supports, respectively, by the self-organization of the sol-derived nano-particles to in situ form mesopores inside macropores of the silica [4]. $\text{CeO}_2\text{--SiO}_2$ was prepared by impregnation of silica Q-50 with $\text{Ce}(\text{NO}_3)_3 \cdot 6\text{H}_2\text{O}$ (KANTO Chemical) aqueous solution followed by calcining at 773 K for 2 h.

Pt supported bimodal catalysts were prepared by incipient-wetness impregnation of bimodal pore supports, with $\text{Pt}(\text{NH}_3)_2(\text{NO}_2)_2$ (Tanaka Co., Pt content: $4.58\text{ wt}\%$) aqueous solution. The impregnated solid was dried at 393 and 773 K for 12 and 2 h, respectively. CeO_2 modified catalysts were prepared by co-impregnation to bimodal pore supports, with a mixture solution of $\text{Pt}(\text{NH}_3)_2(\text{NO}_2)_2$ and $\text{Ce}(\text{NO}_3)_3 \cdot 6\text{H}_2\text{O}$, followed by drying at 393 K for 12 h and calcining at 773 K for 2 h.

2.2. Catalytic reactions

The catalytic reaction was performed in fixed-bed quartz reactor under atmospheric pressure at 973 K . Prior to reaction, 0.1 g of catalyst was reduced at 773 K for 1 h under a flow of pure hydrogen of 40 ml/min . A reactant gas stream that consisted of CH_4 , CO_2 and Ar, with a molar ratio of $5:5:1$ was used. The W/F was fixed at 0.5 or 1 g-cat. h/mol . The effluent gases being cooled through an ice trap were analyzed with two online gas chromatographs. H_2 was analyzed by Shimadzu GC-8A equipped a TCD. CO , CO_2 and CH_4 were analyzed by Shimadzu GC-14B with a TCD. Two Carbosphere columns were used to achieve the separation of H_2 , CO , CO_2 and CH_4 .

2.3. Catalyst characterization

The specific surface area (BET area), pore size distribution and pore volume were determined by nitrogen physical adsorption method on Quantachrome Autosorb-1 instrument (Yuasa Ionics).

The XRD patterns were recorded using a Rigaku RINT2000 diffractometer with $\text{Cu K}\alpha$ radiation in the range of 2θ angles $20\text{--}80^\circ$. Turn over frequency (TOF) values were calculated based on Pt particle sizes with the following equation:

$$\text{TOF} = \frac{r\text{CH}_4 \text{ or } r\text{CO}_2 d}{1.1 n_{\text{Pt}}} \quad (2)$$

where $r\text{CH}_4$, or $r\text{CO}_2$ is CH_4 or CO_2 consumption rate (mol s^{-1} , after 2 h reaction), respectively, n_{Pt} is molar of Pt, and d is diameter of Pt particle size.

3. Results and discussion

3.1. Synthesis and characterization of bimodal pore support

A support with a distinct bimodal pore structure will facilitate solid catalytic reaction. Because the macropores provide a rapid channel for reactant to access the active phase and a fast passage for resultant diffusion from the interior of the pellet to the pore mouth at the external surface of a catalyst. $\text{SiO}_2\text{--SiO}_2$, $\text{ZrO}_2\text{--SiO}_2$ and $\text{Al}_2\text{O}_3\text{--SiO}_2$ bimodal pore supports have been successfully prepared by our group [3,5,6]. In the present work, the synthesis variables for bimodal pore preparation were extensively studied to find the optimal preparation condition for this kind of support. The synthesis conditions and the surface properties of obtained supports are summarized in Table 1. $\text{SiO}_2\text{--SiO}_2$ supports were prepared by incipient-wetness impregnation (IWI) of silica Q-50 with silica sol. Because the viscosity of used silica sol is high, an excess of diluted impregnation solution with respect to the pore volume of the Q-50 was used to make the silica nano-particles easily enter the pores of silica Q-50. But it was divided to several times to keep IWI-type impregnation. For example, the total pore volume of the Q-50 silica pellet was V_s . We diluted the original silica sol with the volume of V_s to $2V_s$. The diluted $2V_s$ sol was impregnated three times; $0.9V_s$, $0.6V_s$, $0.5V_s$, separately, to ensure each time as incipient-wetness impregnation mode. After each time, it was calcined before being used to the successive impregnation. $\text{SiO}_2\text{--SiO}_2^A$, $\text{SiO}_2\text{--SiO}_2^B$ was prepared by three or five successive IWI procedures. In both cases, bimodal pore structure was obtained by calcining the impregnated solids at 873 K for 2 h. The BET surface areas of $\text{SiO}_2\text{--SiO}_2^A$ and $\text{SiO}_2\text{--SiO}_2^B$ were 156 and $134\text{ m}^2/\text{g}$. It seemed that the BET surface area tended to decrease when the impregnation times was more. It should also be noted that the impregnated solids were calcined at 873 K directly without drying. It was believed that it was easy for silica nano-particles aggregating to develop mesopores, when in presence of water vapor during the calcination process [9]. TGA-DTA curves [10] of silica bimodal calcination suggested

Table 1
Characteristics of various supports.

Notation	Synthesis conditions			Surface properties		
	Introduced oxide precursor	SiO ₂ , ZrO ₂ or Al ₂ O ₃ loading (wt%)	Calcined condition	BET (m ² /g)	Pore size (nm)	Pore volume (ml/g)
SiO ₂ (Q-50)	–	–	–	94	59	1.35
SiO ₂ –SiO ₂ ^a	SiO ₂ sol	20	873 K 2 h	156	5.2–55	0.81
SiO ₂ –SiO ₂ ^b	SiO ₂ sol	20	873 K 2 h	134	5.4–56	0.79
ZrO ₂ –SiO ₂ ^a	ZrO ₂ sol	20	673 K 2 h	308	3.7–52	0.70
ZrO ₂ –SiO ₂ ^b	ZrO(NO ₃) ₂ ·2H ₂ O	20	673 K 2 h	119	56.3	0.78
Al ₂ O ₃ –SiO ₂ ^a	Al ₂ O ₃ sol	5	773 K 2 h	86	58.5	1.33
Al ₂ O ₃ –SiO ₂ ^b	Al ₂ O ₃ sol	10	773 K 2 h	100	8.2–57.5	1.33
Al ₂ O ₃ –SiO ₂ ^c	Al ₂ O ₃ sol	20	773 K 2 h	144	8.0–57	1.30
Al ₂ O ₃ –SiO ₂ ^d	Al ₂ O ₃ sol	35	773 K 2 h	120.8	7.4–56	1.20
CeO ₂ –SiO ₂ ^a	Ce(NO ₃) ₃ ·6H ₂ O	10	773 K 2 h	79.5	57	1.1
CeO ₂ –SiO ₂ ^b	Ce(NO ₃) ₃ ·6H ₂ O	20	773 K 2 h	82.0	58.4	1.0

^a Repeated 3 times incipient-wetness impregnation.

^b Repeated 5 times incipient-wetness impregnation.

that the dehydration of silanol groups of the silica nano-particles occurred in the temperature range of 727–800 K. So, the impregnated solids were calcined at 873 K for 2 h directly to generate the silica mesopores by self-assembly of nano-sized SiO₂ from its sol in this study.

For ZrO₂–SiO₂ support, it was indicated that bimodal pore structure could only be formed by impregnating of silica Q-50 with ZrO₂ sol. When using ZrO(NO₃)₂·2H₂O as precursor, the obtained support showed increased BET surface, but, there were no mesopores observed. The effect of Al₂O₃ loading on the surface properties of the obtained support was also investigated. It was found that when the Al₂O₃ loading was 5 wt%, there were just macropores from silica Q-50. When the loading of Al₂O₃ exceeded 10 wt%, Al₂O₃–SiO₂ support with distinct bimodal pore structure was formed. Although Al₂O₃–SiO₂ with 20 wt% Al₂O₃ loading showed larger BET surface area than Al₂O₃–SiO₂ with 10 wt% Al₂O₃ loading, the pore size distribution and pore volume were almost the same. When increasing the Al₂O₃ loading up 35 wt%, the obtained Al₂O₃–SiO₂ support still exhibited bimodal pore structure, but both the BET surface area and pore volume decreased. It was indicated if the Al₂O₃ loading was too large, some of the pores might be blocked and the BET surface area as well as pore volume decreased accordingly. Very interestingly, aluminum nitrate aqueous solution was also employed to prepare bimodal pore support using the same procedure as that of impregnation with alumina sol, but, bimodal pore structure was not obtained (its surface property is not listed in Table 1).

The CeO₂–SiO₂ support showed decreased BET surface area, pore size and pore volume, when compared with the original silica Q-50. It was suggested that CeO₂ blocked some macropores of silica Q-50. For both CeO₂–SiO₂ supports with 10 and 20 wt% CeO₂ loading, bimodal pore structure was not available. It was concluded that SiO₂–SiO₂, ZrO₂–SiO₂ and Al₂O₃–SiO₂ bimodal pore supports could be prepared by impregnation of silica Q-50 gel with SiO₂, ZrO₂ and Al₂O₃ sol, respectively. The optimal preparation condition for SiO₂–SiO₂ bimodal pore support was: three times IWI followed by calcined at 873 K for 2 h without drying. ZrO₂–SiO₂ bimodal pore was obtained after calcining impregnated solid at 673 K for 2 h. To get Al₂O₃–SiO₂ bimodal pore support, Al₂O₃ loading over 10 wt% and calcination at 773 K for 2 h were necessary.

For the convenience of comparison, the loading of alumina, zirconia or additional silica was fixed at 20 wt% for Al₂O₃–SiO₂, ZrO₂–SiO₂ or SiO₂–SiO₂ bimodal pore support. The pore size distributions of the studied bimodal pore supports are given in Fig. 1. It was observed that for all the as-prepared bimodal pore supports, two kinds of pores co-existed. The small pore was in the range of mesopores and the large pore was in the range of macropores but smaller than the original diameter of silica Q-50 pores (59 nm). Combining the surface properties (Table 1) with pore

size distribution of as-prepared bimodal supports, it is inferred that the precursor sol entered the macropores of silica Q-50, the nano-particles from sols aggregated to generate mesopores during the calcination. The newly formed mesopores contributed to the increased BET surface area compared with that of silica Q-50. The bimodal pore structures had been directly observed by field emission scanning electron microscope (FE-SEM) and transmission electron microscopy (TEM) in our previous studies [11,12]. Moreover, because of physicochemical property differences of each sol, the different bimodal pore supports showed varied surface properties.

3.2. The reforming activity of different bimodal pore catalysts

Platinum supported bimodal pore catalysts were applied to CH₄ dry reforming reaction. It was proved by our recent work that Pt-based SiO₂–SiO₂ bimodal pore catalyst was more active than Pt-based unimodal pore catalyst, due to the increased active surface area and high intra-pellet diffusion efficiency facilitated by bimodal pore structure. Here, the activity of different bimodal pore catalyst, including those with hetero-atom combination structure, was compared. TOF values of different bimodal pore catalyst are given in Fig. 2. It is evident that for both CH₄ and CO₂ conversions, the TOF value increases in the following sequence: Pt/SiO₂–SiO₂ < Pt/ZrO₂–SiO₂ ≈ Pt/Al₂O₃–SiO₂, which means that Al₂O₃ and ZrO₂ bimodal catalysts show higher specific activi-

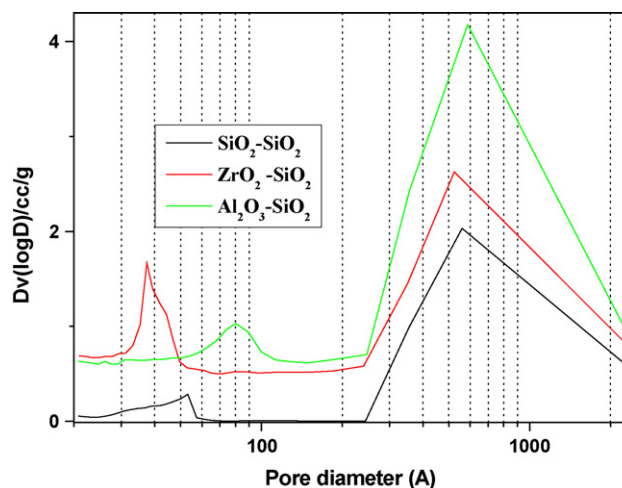


Fig. 1. Pore size distributions of SiO₂–SiO₂, ZrO₂–SiO₂ and Al₂O₃–SiO₂ bimodal pore support.

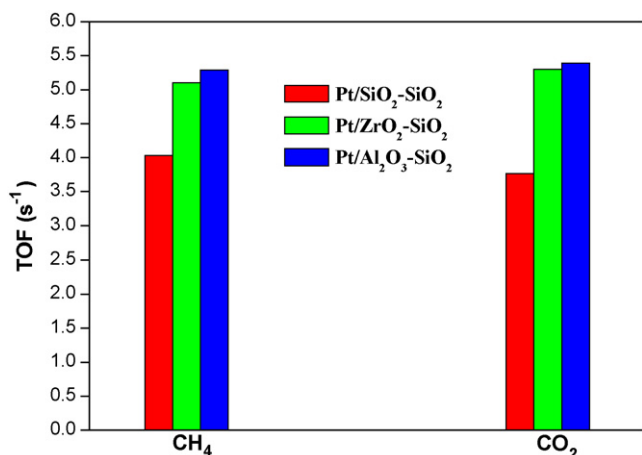


Fig. 2. TOF values for Pt-based bimodal pore catalyst. Pt loading: 3 wt% ($T=973$ K, $P=0.1$ MPa, $W/F=1$ g-cat. h/mol).

ties than SiO₂ only bimodal catalyst. It was believed that besides the spatial effect of bimodal pore structure, introduced Al₂O₃ or ZrO₂ contributed significantly to the reforming activity. Higher TOF values of Pt/ZrO₂-SiO₂ and Pt/Al₂O₃-SiO₂ compared with Pt/SiO₂-SiO₂, indicating these hetero-atom combinations realize promotional effects other pure Pt/SiO₂ interaction, originated from the electronic effect by co-existing ZrO₂ and Al₂O₃, the third component.

3.3. Comparison the performance of ZrO₂ and Al₂O₃ bimodal pore catalysts

Since the performance of ZrO₂ or Al₂O₃ bimodal pore catalyst was better than silica bimodal pore catalyst, in order to obtain a good catalyst for methane dry reforming, the performance of ZrO₂ and Al₂O₃ bimodal pore catalyst were comparatively investigated here. Considering the availability and cost of platinum, it is desirable to develop catalyst with higher activity but lower platinum loading. Fig. 3 compares the reforming activity of ZrO₂ bimodal pore catalyst with Al₂O₃ bimodal pore catalyst at Pt loading of 0.5 and 3 wt%. It was indicated that when reduced the Pt loading from 3 to 0.5 wt%, the reforming activity of ZrO₂ and Al₂O₃ bimodal catalyst both decreased. But, the methane conversion over ZrO₂ bimodal pore catalyst had fallen significantly from 67.4% to 23%, while the activity of Al₂O₃ bimodal pore catalyst declined

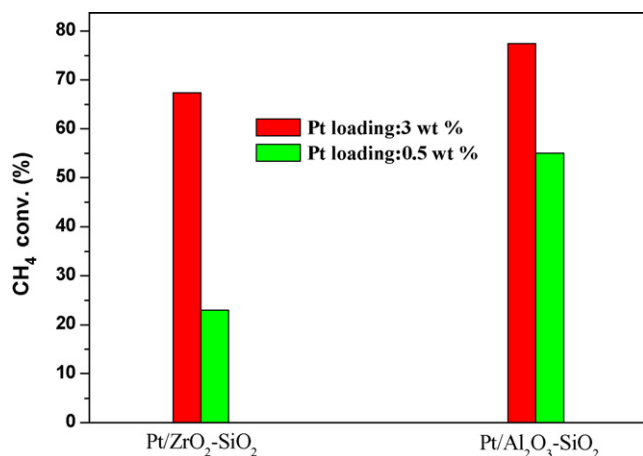


Fig. 3. Effect of Pt loading on reforming activity over Pt/ZrO₂-SiO₂ and Pt/Al₂O₃-SiO₂ bimodal pore catalyst ($T=973$ K, $P=0.1$ MPa, $W/F=1$ g-cat. h/mol).

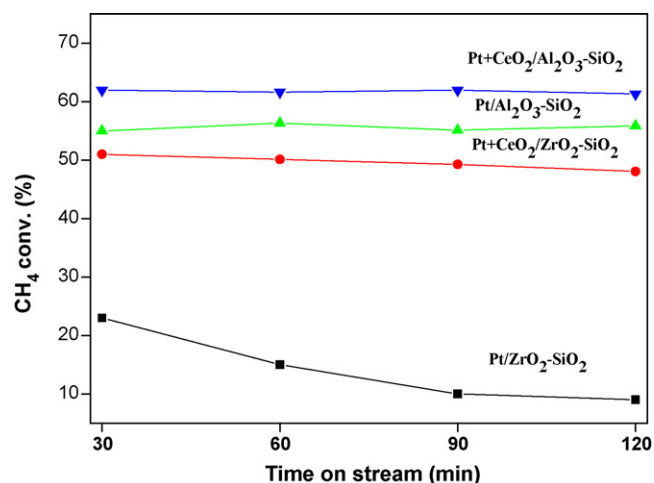


Fig. 4. The promotional effect of Ce on reforming activity over Pt/ZrO₂-SiO₂ and Pt/Al₂O₃-SiO₂ bimodal pore catalyst ($T=973$ K, $P=0.1$ MPa, $W/F=1$ g-cat. h/mol).

slowly. Al₂O₃ bimodal pore catalyst showed higher activity than ZrO₂ bimodal pore catalyst when Pt loading was 0.5 wt%, while two kinds of catalyst exhibited almost the same activity at 3 wt% Pt loading.

Ceria has attracted much attention as an effective promoter for reforming catalysts due to its oxygen storage capacity (OSC). Moreover, it may improve catalytic performances by increasing metal dispersion [13]. To further improve the performance of ZrO₂ and Al₂O₃ bimodal pore catalyst, 10 wt% CeO₂ was co-impregnated with Pt. The dry reforming activity of ZrO₂, Al₂O₃ bimodal pore catalyst and CeO₂-promoted ones is indicated in Fig. 4. It can be seen from Fig. 4 that the ZrO₂ and Al₂O₃ bimodal pore catalyst showed markedly increased activity after being modified by CeO₂. Among all the four catalysts, Pt+CeO₂/Al₂O₃-SiO₂ bimodal pore catalyst exhibited highest reforming activity. To improve process efficiency and downsize the scale of reformer of GTL plant, it is of great importance to development methane reforming catalyst with high activity at high flow rate (low W/F). Fig. 5 compares the reforming activity of Al₂O₃ and ZrO₂ bimodal pore catalyst at $W/F=0.5$ and 1 g-cat. h/mol. When the W/F fell from 1 to 0.5 g-cat. h/mol, the activity of ZrO₂ bimodal catalyst declined sharply and the catalyst deactivated quickly after 1 h reaction. For Al₂O₃ bimodal pore catalyst, the activity was also decreased when the W/F fell to 0.5 g-

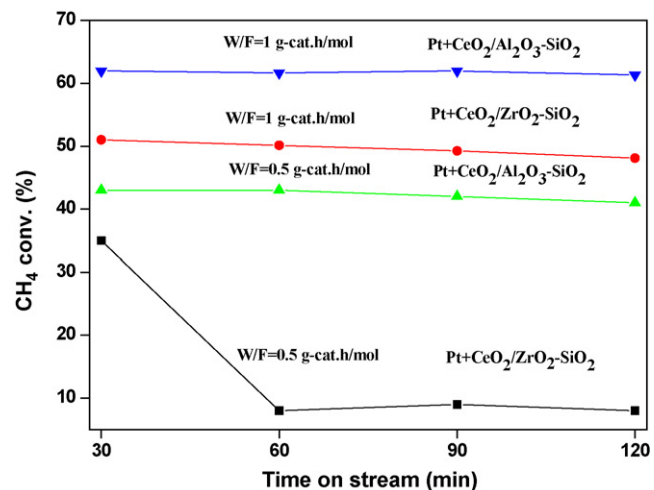


Fig. 5. Comparison of the reforming performance at different W/F ($T=973$ K, $P=0.1$ MPa).

Table 2
Surface properties of studied Pt-based bimodal pore catalysts.

Catalyst ^a	BET (m ² /g)	Support BET (m ² /g)	Pore size (nm)	Pore volume (ml/g)
Pt/ZrO ₂ -SiO ₂	225.3	308	3.5–51	0.68
Pt + CeO ₂ /ZrO ₂ -SiO ₂	279.8	308	4.2–50.5	0.70
Pt/Al ₂ O ₃ -SiO ₂	111.1	144	7.0–57	1.10
Pt + CeO ₂ /Al ₂ O ₃ -SiO ₂	108.8	144	6.8–56.8	0.94

^a Pt and CeO₂ loading were 0.5 and 10 wt%, respectively.

cat. h/mol. But, the activity was still stable at W/F = 0.5 g-cat. h/mol and no obvious deactivation was observed.

The surface properties of 0.5 wt% Pt/ZrO₂-SiO₂, 0.5 wt% Pt/Al₂O₃-SiO₂ and CeO₂ modified ones are summarized in Table 2. It is suggested that the bimodal pore structure was maintained even after loading of both Pt and CeO₂. ZrO₂ bimodal pore catalyst showed increased surface area after being modified by co-existing CeO₂. It was believed that the affinity and interaction between CeO₂ and ZrO₂ can lead to increased surface area, especially, when Ce_xZr_{1-x}O₂ solid solution was formed [14,15]. The BET area of Al₂O₃ bimodal pore catalyst kept almost unchanged by adding CeO₂. The BET surface of ZrO₂ bimodal pore catalyst was larger than Al₂O₃ bimodal pore catalyst, which was in accordance with the surface area of the bimodal pore supports in Table 1.

It was noted that although the surface area of Al₂O₃ bimodal pore catalyst was smaller than that of ZrO₂ bimodal pore catalyst, Al₂O₃ bimodal pore catalyst exhibited better reforming performance. CO chemisorption revealed that active metal surface area and CO monolayer uptake of 3 wt% Pt/Al₂O₃-SiO₂ and 3 wt% Pt/ZrO₂-SiO₂ were: 2.30 m²/g, 47.7 μmol/g, 2.25 m²/g, and 46.7 μmol/g, respectively. The strong interaction between platinum and alumina precursor led to higher Pt dispersion. Furthermore, the pore diameters of Al₂O₃-SiO₂ and ZrO₂-SiO₂ bimodal support were: 8.0–57 and 3.7–52 nm, respectively. The intra-pellet resistance of Al₂O₃-SiO₂ was smaller than that of ZrO₂-SiO₂. It was referred that larger active metal surface area and smaller diffusion resistance both contributed to the higher reforming activity of Pt/Al₂O₃-SiO₂ catalyst, compared with that of Pt/ZrO₂-SiO₂.

The XRD patterns of Pt-based bimodal pore catalysts are shown in Fig. 6. For all bimodal pore catalysts, there were no Pt peaks observed because of the well dispersed Pt particle was too small to be detected by XRD, due to its low content. There were no ZrO₂ peaks in the XRD pattern of ZrO₂ bimodal pore catalyst indicating the highly dispersed ZrO₂ phase. Possibly a part of Zr⁴⁺ strongly interacted with CeO₂ and partially substituted lattice Ce⁴⁺, which

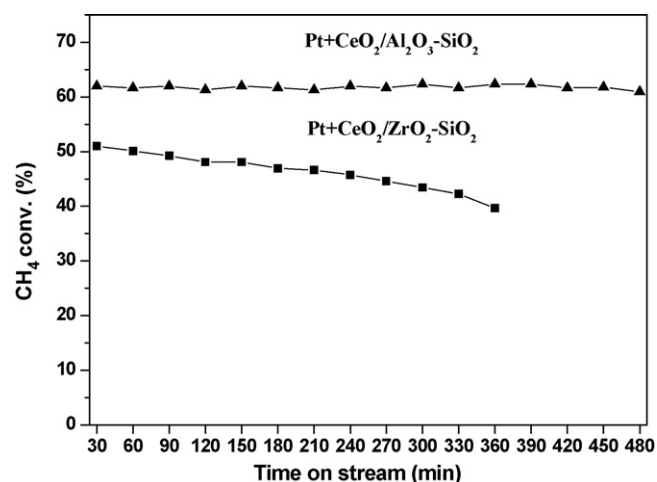


Fig. 7. Stability of Pt + CeO₂/ZrO₂-SiO₂ and Pt + CeO₂/Al₂O₃-SiO₂ catalyst ($T = 973$ K, $W/F = 1$ g-cat. h/mol, Pt loading: 0.5 wt%).

led to increased surface area, in case of Pt + CeO₂/ZrO₂-SiO₂ catalyst. Two characteristic peaks of alumina were found in XRD patterns of Al₂O₃ bimodal pore catalyst. Diffraction peaks at $2\theta = 28.6^\circ$, 33.1° , 47.5° , and 56.3° could be assigned to CeO₂ in XRD profiles of CeO₂ promoted bimodal pore catalysts.

The stabilities of 0.5 wt% Pt + CeO₂/ZrO₂-SiO₂ and 0.5 wt% Pt + CeO₂/Al₂O₃-SiO₂ bimodal pore catalyst are examined in Fig. 7. The ZrO₂ bimodal pore catalyst displayed a rapid drop of catalytic activity. The CH₄ conversion decreased from 51% to 40% in 6 h reaction on stream. However, the Pt + CeO₂/Al₂O₃-SiO₂ bimodal pore catalyst showed a high stability and the CH₄ conversion did not show any drop even after 8 h reaction on stream under the condition of present work.

In conclusion, Al₂O₃ bimodal pore showed better reforming performance compared with ZrO₂ bimodal pore catalyst, especially after further CeO₂ modification.

4. Conclusions

The optimal preparation condition for SiO₂-SiO₂ bimodal pore support is: repeating 3 times incipient-wetness impregnation followed by calcining at 873 K for 2 h without drying. ZrO₂-SiO₂ bimodal pore was obtained after calcining impregnated solid at 673 K for 2 h. To get Al₂O₃-SiO₂ bimodal pore support, Al₂O₃ loading over 10 wt% and calcination at 773 K for 2 h were needed.

The obtained bimodal pore supports showed two kinds of pores, mesopores and original macropores, simultaneously. The newly formed mesopores contributed to the increased BET surface area of bimodal pore support, compared with that of original silica Q-50.

Pt supported on these kinds of supports showed high activity due to the spatial effect of bimodal pore structure and chemical effect from the introduced and embedded hetero-oxides. Pt/Al₂O₃-SiO₂ bimodal catalyst showed better reforming performance than Pt/ZrO₂-SiO₂ bimodal catalyst while CeO₂ modified

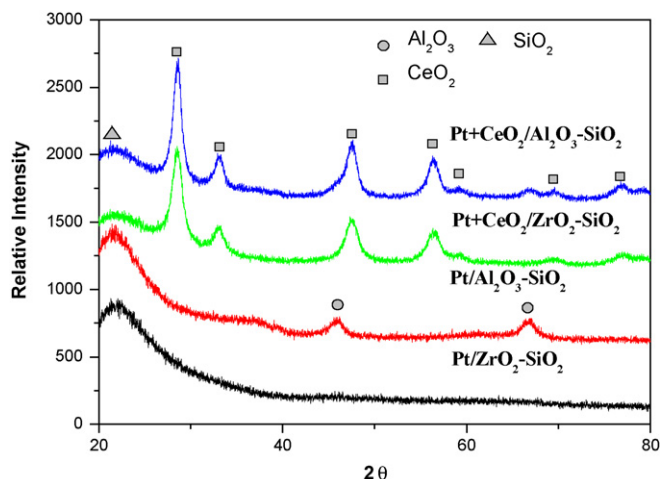


Fig. 6. XRD patterns of studied bimodal pore catalyst. Pt loading: 0.5 wt%.

Pt/Al₂O₃–SiO₂ bimodal pore catalyst exhibited highest activity and stability under the present experimental conditions.

Acknowledgement

Yi Zhang received support from the Foundation of State Key Laboratory of Coal Conversion (No. 10-11-902-1)

References

- [1] T. Inui, M. Funabiki, M. Suehiro, T. Sezume, J. Chem. Soc. Faraday I 75 (1979) 787.
- [2] M. Inoue, K. Kitamura, T. Iui, J. Chem. Tech. Biotechnol. 46 (1989) 233.
- [3] N. Tsubaki, Y. Zhang, S. Sun, H. Mori, Y. Yoneyama, X. Li, K. Fujimoto, Catal. Commun. 2 (2001) 311–315.
- [4] B. Xu, Y. Fan, Y. Zhang, N. Tsubaki, AIChE J. 51 (2005) 2068–2076.
- [5] M. Shinoda, Y. Zhang, Y. Yoneyama, K. Hasegawa, N. Tsubaki, Fuel Process. Technol. 86 (2004) 73–85.
- [6] Y. Zhang, M. Koike, N. Tsubaki, Catal. Lett. 91 (2005) 193–198.
- [7] K. Tomishige, Y.G. Chen, K. Fujimoto, J. Catal. 181 (1999) 91.
- [8] S. Damyanova, B. Pawelec, K. Arishtirova, M.V. Martinez Huerta, J.L.G. Fierro, Appl. Catal. B 89 (2009) 149–159.
- [9] R. Iler, Colloid Chemistry of Silica and Silicates, Cornell University Press, 1955.
- [10] Y. Zhang, M. Shinoda, N. Tsubaki, Catal. Today 93–95 (2004) 55–63.
- [11] Y. Zhang, N. Tsubaki, R. Yang, K. Matsuda, S. Ikeno, J. Nanosci. Nanotechnol. 9 (2009) 3866–3871.
- [12] Y. Zhang, J. Bao, S. Nagamori, N. Tsubaki, Appl. Catal. A 352 (2009) 277–281.
- [13] P. Bera, K.C. Rati, V. Jayaram, G.N. Sublanna, M.S. Hegde, J. Catal. 196 (2000) 293.
- [14] H.-S. Roh, H.S. Potdar, K.-W. Jun, J.-W. Kim, Y.-S. Oh, Appl. Catal. A 276 (2004) 231–239.
- [15] H.-S. Roh, H.S. Potadar, K.-W. Jun, Catal. Today 93–95 (2004) 39–44.